

A phosphotransacetylase from uropathogenic *Staphylococcus saprophyticus*: Characterization, kinetic analysis and its allosteric inhibition by α -ketoglutarate

[*Staphylococcus saprophyticus* Fosfotransasetilaz: Karakterizasyonu, kinetik analizi ve α -ketoglutarat ile allosterik inhibisyonu]

Hamdi Yıldız,
İlknur Yurtsever Aksoy,
Ali Türkan

Department of Chemistry, Faculty of Science,
Gebze Institute of Technology, Kocaeli, TURKEY.

Yazışma Adresi
[Correspondence Address]

Ali Türkan

Department of Chemistry, Faculty of Science, Gebze Institute of Technology, 41400 Çayırova, Kocaeli, TURKEY.
Tel. +90-262-605 3056
Fax. +90-262-605 3101
E-mail: a.turkan@gyte.edu.tr

Registered: 24 February 2012; Accepted: 25 April 2012

[Kayıt Tarihi : 24 Şubat 2012; Kabul Tarihi : 25 Nisan 2012]

ABSTRACT

Objectives: The genome of *Staphylococcus saprophyticus*, an uropathogen, contains SSP2124 gene encoding a putative phosphotransacetylase (Pta). Pta plays significant role in energy metabolism as well as colonization of uropathogens. In this study, cloning, expression, characterization and kinetic analysis of *S. saprophyticus* Pta have been undertaken.

Methods: The SSP2124 gene was amplified by PCR from the genome of *S. saprophyticus* and subcloned into pET28a(+) vector and expressed in *E. coli* BL21. The recombinant Pta was affinity purified by Ni-NTA column. Its characterization as well as its steady-state kinetic analysis has been studied by standard procedures.

Results: The recombinant Pta forms dimers as determined by gel filtration. The activity of the enzyme was maximal at a temperature range of 30-35 °C and at the pH range of 7.5-8.5. It was greatly stimulated by K^+ and NH_4^+ ions, but inhibited by Na^+ ion. Kinetic analysis and product inhibition studies suggest that there is a kinetic mechanism that proceeds through random addition of both substrates to the enzyme before any product is released. The enzyme was inhibited in both acetyl-CoA-forming (forward) and acetyl phosphate-forming (reverse) directions by adenosine triphosphate (ATP) and α -ketoglutarate but not affected by pyruvate and reduced nicotinamide adenine dinucleotide. ATP was competitive with respect to CoA and noncompetitive with respect to acetyl phosphate. The inhibition by α -ketoglutarate, on the other hand, was allosteric with half-saturations at 6.5 ± 0.7 mM and Hill coefficients of 2.6 ± 0.8 and 3.3 ± 0.2 , in forward and reverse directions, respectively.

Conclusions: *S. saprophyticus* Pta belongs to the Pta I family and show similar biochemical features as well as kinetic mechanism with other members. And the most importantly, this study presents the first example of allosteric regulation of a member of class I Ptas.

The authors do not have a conflict of interest.

Keywords: Phosphotransacetylase, *Staphylococcus saprophyticus*, the *eutD* gene, kinetic analysis, α -ketoglutarate, allosteric inhibition.

ÖZET

Amaç: Bir üropatojen olan *Staphylococcus saprophyticus* genomu putatif Fosfotransasetilaz (Pta) kodlayan SSP2124 genini içermektedir. Pta üropatojenlerin enerji metabolizmasında ve üriner sistemde kolonize olmalarında önemli bir rol oynamaktadır. Bu çalışmada, *S. saprophyticus* Pta'nın klonlanması, ekspresyonu ve biyokimyasal karakterizasyonu yapıldıktan sonra kinetik mekanizması aydınlatılmıştır.

Yöntem: SSP2124 geni PCR ile *S. saprophyticus* genomundan çoğaltıldı ve pET28a(+) vektörüne klonlandı ve *E. coli* BL21'de ekspres edildi. Rekombinant enzim Ni-NTA afinite kolonu ile saflaştırılıp, karakterizasyon ve kinetik analiz çalışmaları standart prosedürlere göre yapılmıştır.

Bulgular: Rekombinant Pta'nın dimer oluşturduğu jel filtrasyon ile belirlenmiştir. Enzimin aktivitesi 30-35°C ve 7.5-8.5 pH aralığında maksimum seviyededir. K^+ and NH_4^+ iyonları enzim aktivitesini artırmakta, fakat Na^+ iyonu inhibe etmektedir. Kinetik analiz ve ürün inhibisyon çalışmaları, enzimin herhangi bir ürün salınımı gerçekleşmeden önce her iki substratın rastgele enzime eklendiği üçlü kompleks oluşan bir mekanizmaya sahip olduğunu göstermiştir. Adenozin trifosfat (ATP) ve α -ketoglutarat Pta aktivitesini hem ileri hem de geri yönde inhibe ederken, piruvat ve nikotinamid adenin dinükleotid aktiviteye etki etmemektedir. ATP, koenzim A'ya karşı kompetitif inhibitör iken, asetil-fosfata karşı nonkompetitif bir inhibitördür. α -Ketoglutarat ise allosterik bir inhibitör olup, yarı-doygunluk değeri 6.5 ± 0.7 mM ve Hill katsayısı, ileri ve geri reaksiyon için sırasıyla, 2.6 ± 0.8 and 3.3 ± 0.2 hesaplanmıştır.

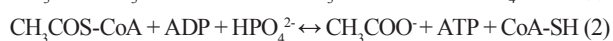
Sonuç: *S. saprophyticus* Pta, sınıf-I Pta üyesi olup, biyokimyasal özellikleri ve kinetik mekanizması diğer üyelerinkine benzerlik göstermektedir. En önemlisi, bu çalışma, bir Pta I üyesinin allosterik regülasyona tâbi olduğunun ilk örneğini göstermektedir.

Yazarların çıkar çatışması bulunmamaktadır.

Anahtar Sözcükler: Fosfotransasetilaz, *Staphylococcus saprophyticus*, *eutD* geni, kinetik analiz, α -ketoglutarat, allosterik inhibisyon.

Introduction

Phosphotransacetylase (Pta; EC 2.3.1.8) is a ubiquitous enzyme and plays an integral role in acetate metabolism along with acetate kinase (AckA; EC 2.7.2.1) in diverse fermentative microbes belonging to the domain of *Bacteria* [1]. Pta catalyzes reversible transfer of acetyl group from acetyl phosphate (acetyl~P) to coenzyme A (CoA), forming acetyl-coenzyme A (acetyl-CoA) and inorganic phosphate (equation 1). AckA catalyzes the reversible conversion of acetyl~P to acetate coupled to substrate-level phosphorylation of ADP to yield ATP (equation 2). Therefore, Pta-AckA pathway plays a significant role in acetyl~P and acetyl-CoA homeostasis in fermentative microbes [1].



Ptas from different microorganisms share high levels of sequence similarity [2]. So far, two classes of Ptas have been identified: PtaIs and PtaIIs, which are about 350 and 700 residues in length, respectively [3-5]. PtaI is encoded by the *eutD* gene¹. PtaII, on the other hand, is encoded by the *pta* gene, which is organized in a single operon along with the *ackA* gene. PtaIIs contain three conserved domains: the P loop NTPase domain at the N-terminus, a DRTGG domain and the C-terminal domain where active site is located [5, 6]. The C-terminal domain shares high homology with PtaIs. The P loop NTPase domain, on the other hand, acts as a regulatory domain whereby the allosteric effectors, namely NADH, ATP and pyruvate, display their effects on the activity [5, 6]. Unlike PtaIIs, PtaIs have been considered not to be allosterically regulated. The activity of Ptas purified from *Bacillus subtilis* and *Veillonella alcalescens* were shown to be inhibited by the adenine nucleotides, ATP and ADP, but not affected by pyruvate and NADH [7, 8]. To date, the crystal structures of three members of PtaIs from *Methanosarcina thermophila*, *Streptococcus pyogenes* and *B. subtilis* have been determined, but no crystal structure of a PtaII is available yet [2, 9, 10]. All three crystal structures show that the enzyme folds into an α/β architecture with two domains separated by a prominent cleft, which presumably contains the substrate binding sites, and forms a homodimer [2, 9, 10]. Kinetic analyses of the Ptas from *Clostridium kluyveri*, *V. alcalescens* and *M. thermophila*, suggested that the mechanism proceeds through random addition of both substrates to the enzyme before any product is released [8, 11, 12]. Several essential residues for substrate binding in the active site of *M. thermophila* Pta have been identified and a catalytic mechanism has been proposed [13, 14].

Some microorganisms such as *Escherichia coli* and *Salmonella enterica* possess both the *pta* and the

eutD genes (KEGG Database). The *eutD* genes from *S. enterica* and *E. coli* were cloned, characterized and shown to display high Pta activity [4, 15]. Furthermore, in *S. enterica* and *E. coli* *pta* strains, the EutD proteins were shown to compensate for the lack of PtaII activity during growth on acetate [4, 15].

The phosphotransacetylase activity also is of importance for virulence of some pathogenic bacteria. Welch and coworkers indicated that Pta-AckA pathway plays a role in colonization and pathogenesis of uropathogenic *E. coli* CFT073 during murine urinary tract infection (UTI), possibly by providing acetogenic products, acetyl~P and acetyl-CoA [16]. Acetyl~P has been shown to function as a global signal and hence to influence in vivo expression of almost 100 genes in many different microorganisms [for an excellent review see reference 1].

Staphylococcus saprophyticus is a leading gram-positive uropathogen of uncomplicated UTI in young female outpatients [17]. The genome of *S. saprophyticus* contains a gene (SSP2124, although designated as a *eutD* gene *Staphylococcus* species do not have an ethanolamine utilization operon) encoding a putative Pta of 328 residues in length (KEGG Database). It also contains a *ackA* gene (SSP1054) but not located in the same operon with SSP2124. Although based on the DNA sequence it is highly likely that the gene SSP2124 encodes a PtaI, it has not been studied so far.

In this work, we cloned, expressed and characterized the protein product of SSP2124 gene from *S. saprophyticus*. Furthermore, we determined the kinetic mechanism of the recombinant enzyme and investigated the effect of some metabolites involved in the central energy metabolism, namely ATP, NADH, pyruvate and α -ketoglutarate, on the activity of the enzyme.

Experimental Procedures

Materials

Primers were from Integrated DNA Technologies (Iowa, USA). Restriction enzymes were from New England BioLabs Inc. (USA). *pET28a(+)* expression vector was purchased from Merck (Dramstadt, Germany). All chemicals were purchased from Sigma-Aldrich (St. Lois, MO, USA).

Cloning

The SSP2124 gene encoding the putative Pta was amplified from *S. saprophyticus* SSP2124 (DSM 20229, ATCC 15305) genome by PCR using primers 5'-AGGCCCCATATGACTTTATTAGATGTATTACAA-3' (sense)

and 5'-TTGCTAGGATCCTTATTGCAATGATTGTGC-3' (antisense). The start and stop codons for the SSP2124 gene are shown in bold. The restriction enzyme sites *Nde*I (sense) and *Bam*HI (antisense) are shown in italics. The PCR used Paq5000 DNA polymerase (Stratagene), and consisted of a denaturation step (95 °C, 2 min), followed

by 30 cycles of annealing (57 °C, 30 s), extension step (72 °C, 2 min) and denaturation (94 °C, 1 min), and a final extension step (72 °C, 10 min). The PCR product was subcloned into the *pET28a(+)* vector using the *NdeI* and *BamHI* restriction sites. The *pET28a(+)* vector containing the insert (*pET28a(+)-Pta*) was transformed initially into *E. coli* Top10, which was grown in Luria broth containing kanamycin (30 µg/mL). The identity of the insert was confirmed by DNA sequencing.

Protein expression and purification

pET28a(+)-Pta plasmid was transformed into the expression host *E. coli* BL21 (DE3). The cells were grown at 30 °C to an OD₆₀₀ of 0.6-0.8 in Luria broth, followed by induction with isopropyl β-D-1-thiogalactopyranoside (IPTG) (0.25 mM final concentration) and expression overnight at 20 °C. The cells were harvested by centrifugation (6000xg, 4 °C, 10 min) and washed twice with TN buffer (20 mM Tris-HCl, pH 7.5, and 200 mM NaCl). At this point the cells were stored at -80 °C, if not used immediately. The cell pellet was resuspended in ten volumes of lysis buffer (25 mM Tris-HCl, pH 8.0, 200 mM NaCl, 1% Triton X-100, 1 mM dithiothreitol (DTT), 1xEDTA-free Complete Protease Inhibitor Cocktail (Roche), lysozyme (1 mg/1 g wet cells). The cells were disrupted by sonication on ice (twenty times for 15 s, with 1-2 min intervals for cooling on ice) and the resulting lysate was clarified by centrifugation (10000xg, 4 °C, 20 min). The supernatant was added to 2 mL of Ni-NTA resin (Qiagen) prewashed with buffer (25 mM Tris-HCl, pH 8.0, and 200 mM NaCl) in a PD-10 column. The Ni-NTA column was washed with 10 bed volumes of buffer (25 mM Tris-HCl, pH 8.0, 200 mM NaCl, 1% Triton X-100) and then with 10 bed volumes of buffer (25 mM Tris-HCl, pH 8.0, 200 mM NaCl, and 10 mM imidazole). The His₆-Pta was eluted with buffer (25 mM Tris-HCl, pH 8.0, 200 mM NaCl, and 200 mM imidazole) and 1 mL fractions were collected. The fractions containing Pta, as determined by SDS-polyacrylamide gel electrophoresis, were pooled and dialyzed against four changes of 2 L of dialysis buffer (25 mM Tris-HCl, pH 7.5, 50 mM KCl and 1 mM DTT) for 8 h each at 4 °C.

We also tried to remove His-tag by cleaving with thrombin (Sigma-Aldrich, USA), but the activity of the protein was significantly lost. Thus, the following experiments were carried out using His₆-Pta.

Phosphotransacetylase activity assay

Pta activity in the forward direction (acetyl-CoA synthesis) was measured at 25 °C by monitoring the thioester bond formation of acetyl-CoA at 233 nm ($\epsilon_{233\text{ nm}} = 5.55 \text{ mM}^{-1}\text{cm}^{-1}$). The reaction mixture contained 50 mM Tris-HCl (pH 7.5), 150 mM KCl, 3 mM lithium acetyl phosphate, 0.2 mM lithium CoA, 2 mM DTT and enzyme (0.025 µg) in a final volume of 100 µL. The reaction was initiated by addition of the enzyme.

The reverse Pta activity was measured at 25 °C by monitoring the phosphate-dependent CoA release from acetyl-CoA with Ellman's reagent, 5',5-dithiobis(2-nitrobenzoic acid) (DTNB) as the formation of thiophenolate anion at 412 nm ($\epsilon_{412\text{ nm}} = 13.6 \text{ mM}^{-1}\text{cm}^{-1}$). The assay mixture contained 50 mM Tris-HCl (pH 7.5), 150 mM KCl, 0.2 mM DTNB, 10 mM KH₂PO₄ (pH 7.5), 0.2 mM acetyl-CoA and enzyme (0.025 µg) in a final volume of 100 µL. The reaction was initiated by addition of enzyme.

All measurements were performed in 96-well flat-bottomed quartz microtiter plate (Molecular Devices) using a SpectraMax 250 kinetic plate reader (Molecular Devices, Sunnyvale, CA).

Effect of Metabolites

ATP, NADH, pyruvate, and α-ketoglutarate were tested for the effect on the activity of Pta. The enzyme activity was measured in the absence or presence of 1 mM of NADH and ATP, or 10 mM of pyruvate and α-ketoglutarate. In the forward reaction, acetyl~P and CoA concentrations were 500 µM and 200 µM. In the reverse reaction, acetyl-CoA and phosphate concentrations were 125 µM and 4 mM, respectively. Other conditions were as described in "Activity assay" section. The results are presented as the percentages of activity in the presence of the effectors relative to the activity measured in the absence of the metabolites (Fig. 6).

Kinetics analyses

For two-substrate profile analysis of both acetyl-CoA-forming (forward) and acetyl~P-forming (reverse) reactions, initial velocity studies were performed with varying concentrations of one substrate at several fixed concentrations of the corresponding second substrate. Lineweaver-Burk double-reciprocal plots were generated by linear least-square fits of the data (Fig. 4) [18]. The measurements were performed at least in triplicate. Other conditions were as described in "Activity assay" section. The kinetic constants given in Table 1 were determined by globally fitting the data to Equations 6-8 [18]:

For product inhibition experiments, the initial velocities were determined with varying concentrations of one substrate at fixed saturating and subsaturating concentrations of the corresponding second substrate (given in the text) in the absence or presence of indicated fixed concentrations of the product inhibitor (phosphate or acetyl-CoA). The measurements were performed at least in triplicate. Other conditions were as described in "Activity assay" section. Lineweaver-Burk double-reciprocal plots were generated by linear least-square fits of the data (Fig. 5). The data were fitted to equations describing competitive (Equation 3) or noncompetitive (Equation 4) inhibition using two dimensional least-square analysis [18].

$$1/v = K_m/V(1+I/K_i)(1/S) + 1/V \quad (3)$$

$$1/v = K_m/V(1+I/K_i)(1/S) + 1/V(1+I/K_i) \quad (4)$$

where K_m is the Michaelis constant for the substrate, S is the concentration of substrate, I is the concentration of the inhibitor, and K_i is the inhibition constant for the product inhibitor. The calculated K_i values are given in Table 2.

Kinetic analysis of ATP inhibition

For ATP versus CoA, initial velocity measurements were carried out with varying concentrations of CoA at fixed concentration of acetyl~P (500 μ M) in the absence or presence of 1 mM or 2 mM ATP. Data were expressed as double-reciprocal plots (Fig. 7A). For ATP versus acetyl~P, initial velocity measurements were carried out with varying concentrations of acetyl~P at fixed concentration of CoA (200 μ M) in the absence or presence of 1 mM or 2 mM ATP. Data were expressed as double-reciprocal plots (Fig. 7B). Other conditions were as described in "Activity assay" section.

To determine the inhibition constants for ATP binding, initial velocity measurements were carried out with varying concentrations of CoA at several fixed concentrations of acetyl~P (250, 500, 1000 and 2000 μ M) in the absence or presence of 1 mM or 2 mM ATP. The inhibition constants were determined using the equation 5 and the corresponding double-reciprocal and the secondary plots as described [18]:

$$\frac{v}{V_{\max}} = \frac{[A]}{\alpha K_A \left(1 + \frac{K_B}{[B]} + \frac{[I]K_B}{K_i[B]} + \frac{[I]}{\beta K_i} \right) + [A] \left(1 + \frac{\alpha K_B}{[B]} \right)} \quad (5)$$

where V_{\max} is the maximal velocity, A and B are the varied (CoA) and fixed (acetyl~P) substrates, respectively; I is the inhibitor (i.e., ATP); K_A and K_B are the dissociation constants of substrates A and B binding to free enzyme, respectively; the α represents the factor by which the dissociation constant for A is changed by the binding of B (and the factor by which the dissociation constant for B is changed by the binding of A); K_i is the dissociation constants of I; the β represents the factor by which the dissociation constant for B is changed by the binding of I (and the factor by which the dissociation constant for I is changed by the binding of B).

Protein concentration

The protein concentration was determined by bicinchoninic acid (BCA) method [19], using bovine serum albumin (BSA) as a standard.

Gel electrophoresis

SDS-PAGE was performed in 12% (w/v) polyacrylamide gels, according to the method of Laemmli [20]. Electrophoresis was performed at 150 V and 10 °C. Proteins were visualized with Coomassie Blue staining.

Gel filtration chromatography

Gel filtration was performed using a ÄKTA FPLC

system (GE Healthcare, USA) equipped with a Sephacryl 300 16/60 column (GE Healthcare, USA). The column was equilibrated with 50 μ M Tris-HCl, pH 7.5, containing 150 μ M NaCl, and calibrated using molecular mass standards (ferritin (440 kDa), aldolase (158 kDa), conalbumin (75 kDa) and albumin (43 kDa); GE Healthcare, USA). The void volume of the column was determined with Blue Dextran. The sample (1 mg/mL) and the standards (1 mg/mL each) were applied separately in a final volume of 100 μ L at a constant flow rate of 0.5 mL/min.

Data analysis

All data were analyzed by global fitting to the corresponding equations by nonlinear regression using OriginPro software, version 7.0 [OriginLab Corporation, USA].

Results

Initial characterization of recombinant *S. saprophyticus* Pta

S. saprophyticus Pta which has 328 amino acids belongs to the class I Ptas. In this class of Ptas, so far, the crystal structures of *M. thermophila*, *S. pyogens* and *B. subtilis* Ptas have been reported, all of which form homodimers and have very similar folding patterns [2, 9, 10]. BLAST search indicated that *S. saprophyticus* Pta shares 67%, 55% and 45% identity with *B. subtilis*, *S. pyogens* and *M. thermophila* Ptas, respectively. *S. saprophyticus* Pta also possesses the strictly and highly conserved residues (Fig.1). It has extra 5 residues in the loop region connecting α 9 and α 10 helices.

Recombinant *S. saprophyticus* Pta fused to a His-tag was purified using a Ni-NTA column (Fig. 2). A molecular mass of 77 ± 4 kDa was calculated for the recombinant enzyme from gel filtration studies, indicating that the enzyme mostly exists as a dimer. The activity of the enzyme was maximal at a temperature range of 30-35 °C (Fig. 3A), and at the pH range of 7.5-8.5 (Fig. 3B). Maximum Pta activity was dependent on the presence of potassium chloride or ammonium chloride in the assay mixture (Fig. 3C). In the presence of saturated KCl (125 mM), ammonium chloride did not cause further increase in the activity (data not shown), indicating that they share the same binding site. Sodium chloride was inhibitory, a property common to the other known phosphotransacetylases (BRENDA database).

Kinetic analysis of recombinant *S. saprophyticus* Pta

The initial velocity patterns of two-substrate, two-product reaction catalyzed by *S. saprophyticus* Pta were investigated. The enzyme displayed classical Michaelis-Menten saturation kinetics in both acetyl-CoA-forming (forward) and acetyl~P-forming (reverse) directions. For both directions, the data expressed as double-reciprocal

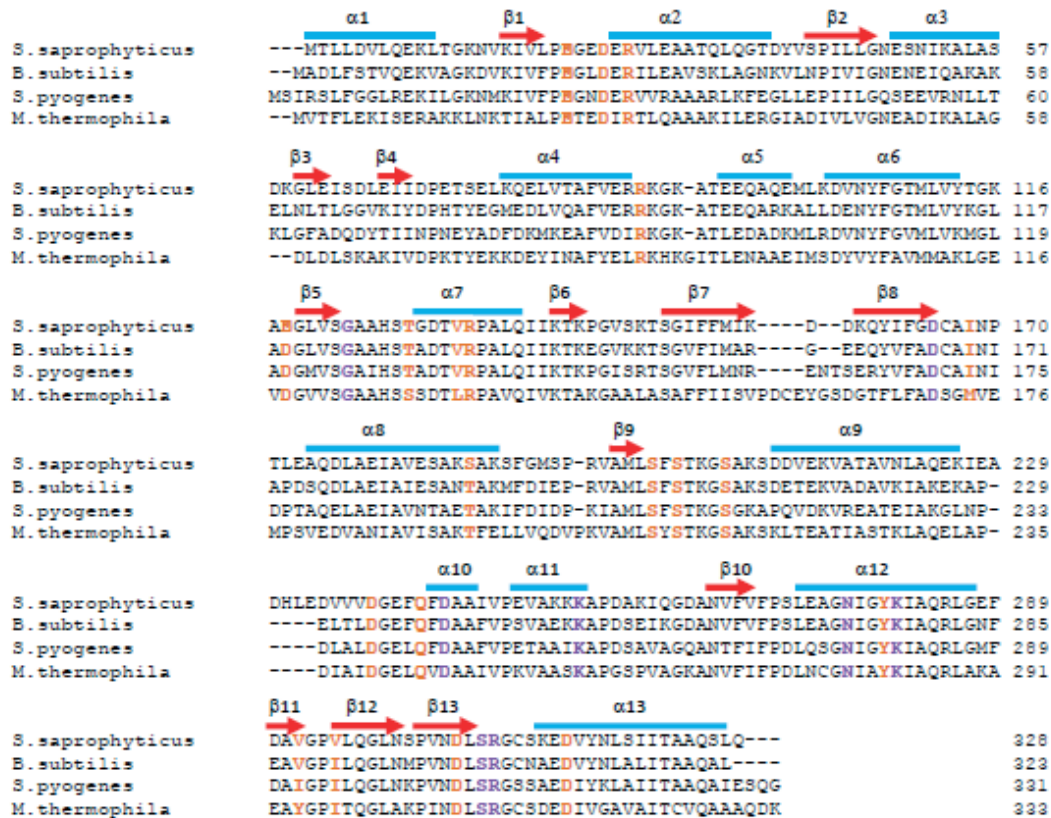


Figure 1. Sequence alignment of *S. saprophyticus* Pta with Ptas from *B. subtilis*, *S. pyogenes* and *M. thermophila*. Blue bars and red arrows above the sequences show, respectively, α -helices and β -strands of the *B. subtilis* Pta. Residues in purple and orange demonstrate the strictly and highly conserved residues, respectively, based on the alignment among 32 prokaryotic Pta sequences made by Iyer et al [2]. Dashes represent gaps.

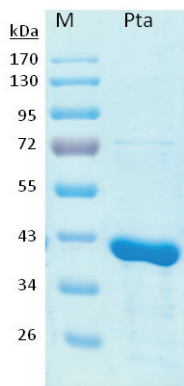


Figure 2. SDS-polyacrylamide gel (12%) electrophoresis of affinity purified recombinant *S. saprophyticus* Pta. M, prestained molecular mass markers (Fermantas); Pta, affinity purified His6-Pta (5 μ g). The gel was stained with Coomassie Brilliant Blue.

plots yielded sets of intersecting lines (Fig. 4), agreeing with a ternary complex kinetic mechanism rather than a ping-pong kinetic mechanism. As explained in detail below, product inhibition patterns suggested that the kinetic mechanism obeys rapid equilibrium random bi bi model (Fig. 5). Therefore, the data were fitted globally to Equations 6-8 describing the pattern for a rapid

equilibrium random bi bi mechanism [18]:

$$\frac{1}{v} = \frac{\alpha K_A}{V_{\max}} \left(1 + \frac{K_B}{[B]} \right) \frac{1}{[A]} + \frac{1}{V_{\max}} \left(1 + \frac{\alpha K_B}{[B]} \right) \quad (6)$$

$$V_{\max}^{app} = \frac{V_{\max}}{\left(1 + \frac{\alpha K_B}{[B]} \right)} \quad (7) \quad \text{and}$$

$$K_A^{app} = \alpha K_A \frac{\left(1 + \frac{K_B}{[B]} \right)}{\left(1 + \frac{\alpha K_B}{[B]} \right)} \quad (8)$$

where V_{\max} is the maximal velocity, A and B are the varied and fixed substrates, respectively, K_A and K_B are the dissociation constants of substrates A and B binding to free enzyme, respectively. The constant α is the ratio of apparent dissociation constants for binding of one

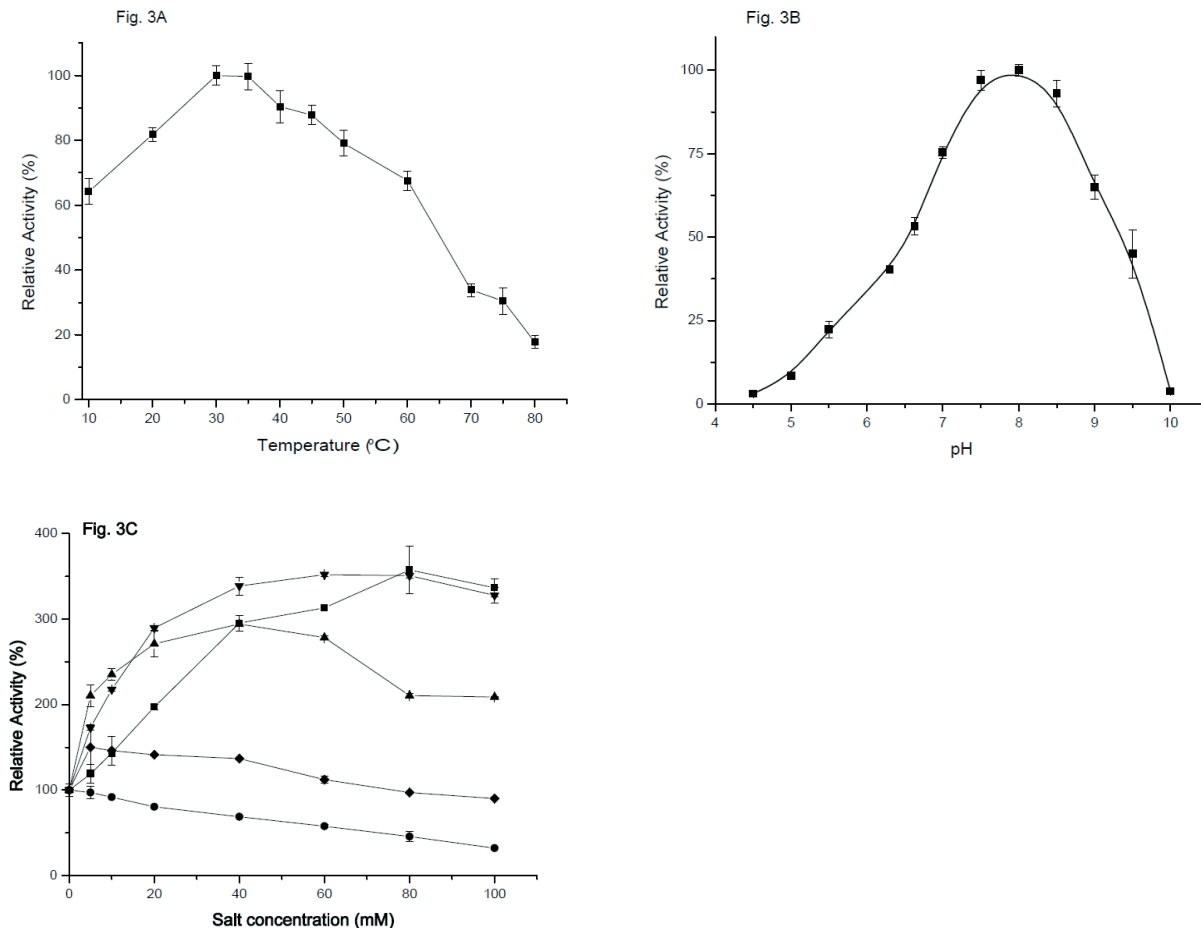


Figure 3. Optimal temperature, pH and salt for recombinant *S. saprophyticus* Pta activity. Profiles were generated for the forward (Acetyl-CoA-forming) reaction as described under “Experimental Procedures”. A, temperature profile with activities normalized to the value at 30 °C, the optimal temperature. B, pH profile with activities normalized to pH 8.0, the maximum value obtained. The buffers used were 50 mM acetate (pH 4.5-5.5), 50 mM MOPS (pH 6.3-7.0), 50 mM Tris-HCl (pH 7.5-9.0), 50 mM glycine (pH 9.5-10.0). KOH or HCl is used to adjust the pHs of the solutions. C, effects of various salts on Pta activity: KCl (■); NH₄Cl (▼); (NH₄)₂SO₄ (▲); NaCl (●); and potassium phosphate, pH 8.0, (◆). Data are presented as relative percent over no added salt. Each assay contained 0.025 μg of protein. 100 % specific activities were about 650 μmoles/min/mg protein in A and B, and 150 μmoles/min/mg protein in C.

substrate in the presence and absence of the second substrate [18]. V_{max}^{app} and K_A^{app} denote apparent V_{max} and K_A , respectively.

Table 1 demonstrates the calculated kinetic constants for the substrates of the forward and reverse reactions catalyzed by Pta. It can be seen from the data that in the forward reaction, αK values for both substrates are larger than their corresponding K values (i.e., $\alpha \approx 4$), indicating that binding of either CoA or acetyl~P first decreases the affinity for the other. In fact, in Figs. 4A and B, the lines look like seemingly parallel and intersect below the $1/[B]$ axes (not shown), also demonstrating that binding of one substrate inhibits the binding of the other (i.e., $\alpha > 1$) [16]. On the other hand, in the reverse reaction binding of one substrate does not significantly affect the binding of the other ($\alpha \approx 1$). In Figs. 4C and D, the lines intersect on the $1/[B]$ axes (not shown), also indicating that $\alpha \approx 1$. In fact, in the reverse reaction K_A^{app} value for either acetyl-CoA or phosphate was constant in the range of experimental

error (i.e., did not significantly change with increasing fixed concentrations of the corresponding second substrate); the K_A^{app} for acetyl-CoA was 130 ± 24 μM and for phosphate was 5.0 ± 0.7 mM. Whereas, in the forward reaction, K_A^{app} value for substrate A increased approximately fourfold with increasing [B]. In this case, K_A^{app} approaches K_A as [B] decreases [18]. At low CoA (25 μM), the K_A^{app} for acetyl~P was 180 ± 41 μM, and at saturating CoA (400 μM), it was 395 ± 60 μM. Similarly, at low acetyl~P (150 μM), K_A^{app} for CoA was 47 ± 12 μM and at saturating acetyl~P (3000 μM), it was 210 ± 17 μM. When [B] is saturating, the value of αK_A is equal to the Michaelis constant for A (i.e., K_m^{app}) [21].

The product inhibition patterns of the reaction catalyzed by Pta were analyzed to determine if substrate binding and product release are random or ordered. Fig. 5 shows double-reciprocal plots of the inhibition of acetyl-CoA-forming reaction catalyzed by Pta by the product inhibitors, inorganic phosphate and acetyl-CoA, at

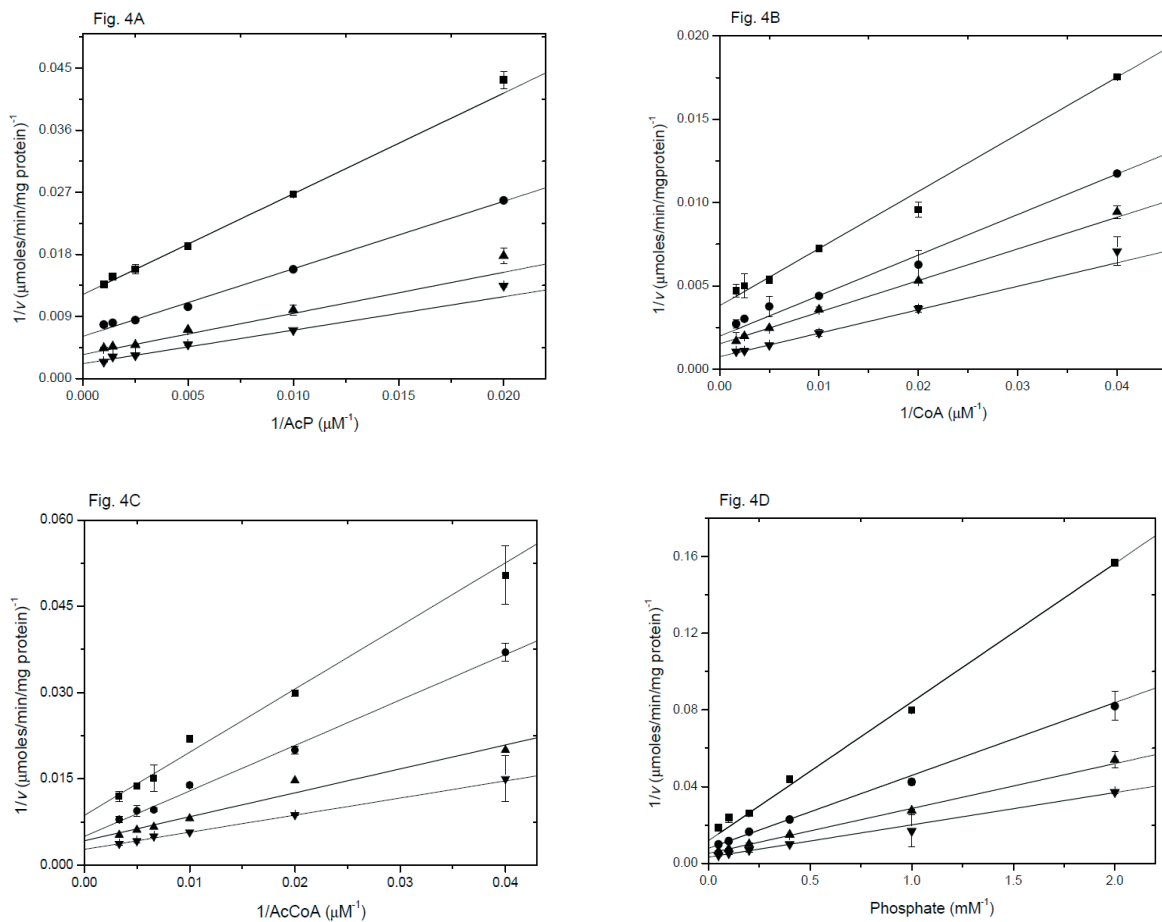


Figure 4. Initial velocity patterns of the forward and reverse reactions catalyzed by *S. saprophyticus* Pta. (A and B) Acetyl-CoA-forming direction: A, The CoA concentration was kept constant at 25 μM (\blacksquare), 50 μM (\bullet), 100 μM (\blacktriangle), and 200 μM (\blacktriangledown); B, Acetyl phosphate (AcP) concentration was kept constant at 150 μM (\blacksquare), 300 μM (\bullet), 500 μM (\blacktriangle), and 3000 μM (\blacktriangledown). (C and D) AcP-forming direction: C, Phosphate concentration was kept constant at 1.0 mM (\blacksquare), 2.5 mM (\bullet), 5.0 mM (\blacktriangle), and 20.0 mM (\blacktriangledown); D, The acetyl-CoA concentration was kept constant at 50 μM (\blacksquare), 100 μM (\bullet), 200 μM (\blacktriangle), and 400 μM (\blacktriangledown). Other conditions as described in the “Experimental procedure” section.

Table 1. Kinetic constants determined using Eqns 6-8 for the forward reaction (acetyl phosphate + CoA \rightarrow acetyl-CoA + phosphate) and reverse reaction (acetyl-CoA + phosphate \rightarrow acetyl phosphate + CoA) of *S. saprophyticus* Pta. The values are given as average \pm standard deviation.

Substrate	K' (μM)	$\alpha K''$ (μM)	k_{cat} (s^{-1})
<i>Forward reaction</i>			
Acetyl phosphate	140 \pm 35	593 \pm 125	1156 \pm 146
CoA	51 \pm 18	235 \pm 48	
<i>Reverse reaction</i>			
Phosphate	4086 \pm 424	5000 \pm 700	397 \pm 26
Acetyl-CoA	130 \pm 24	165 \pm 47	

*Dissociation constant of substrate binding to free Pta.

**Dissociation constant of substrate binding to Pta-second substrate complex.

saturation and subsaturating conditions. Phosphate was a competitive inhibitor with respect to acetyl-P when CoA was at saturating (600 μM) or subsaturating (100 μM) levels (Fig. 5A and B). Phosphate was a noncompetitive inhibitor versus CoA when acetyl-P was at subsaturating (500 μM) (Fig. 5C) but it did not inhibit versus CoA when acetyl-P was at saturating level (4 mM) (data not shown). Acetyl-CoA was a

competitive inhibitor versus CoA when acetyl-P was at subsaturating levels (Fig. 5D), but it did not inhibit versus CoA when acetyl-P was at saturating levels (data not shown). Similarly, acetyl-CoA was a competitive inhibitor with respect to acetyl-P when CoA was at subsaturating levels (Fig. 5E), but it did not inhibit versus acetyl-P when CoA was at saturating levels (data not shown). The inhibition constants, K_i values,

for the product inhibitors are given in Table 2. These patterns of inhibition are very similar to that obtained for *M. thermophila* Pta [12] and diagnostic for a kinetic mechanism that proceeds through formation of a ternary complex in which the substrates can bind to the enzyme in random order [12, 18].

Effect of metabolites on the activity of *S. saprophyticus* Pta

ATP, NADH, pyruvate, and α -ketoglutarate were tested for the effect on the activity of *S. saprophyticus* Pta in both forward (acetyl-CoA-forming) and reverse (acetyl

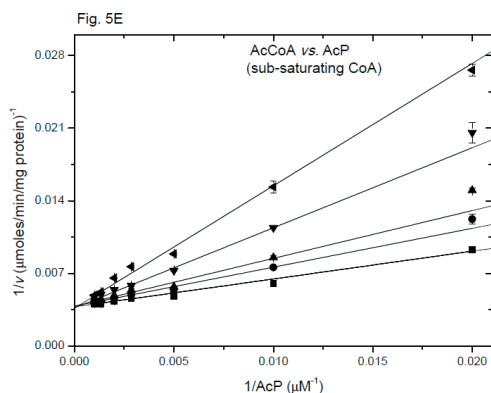
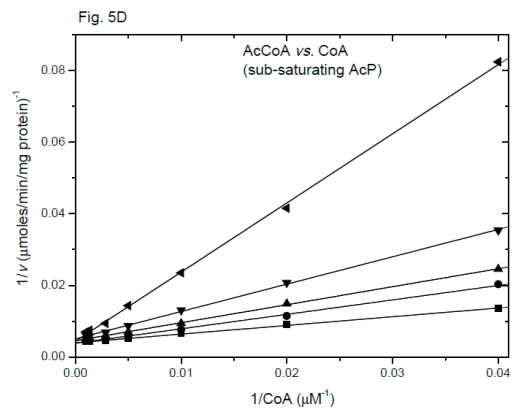
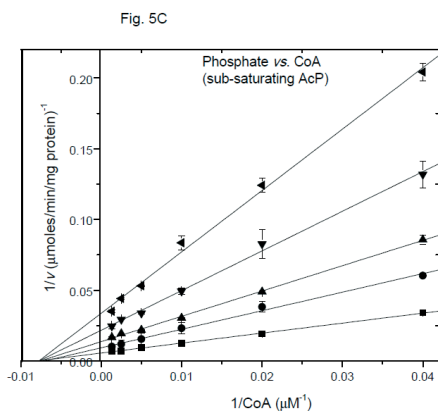
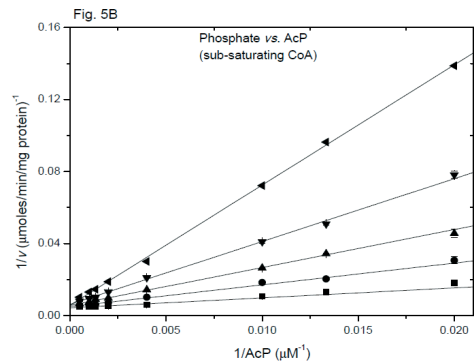
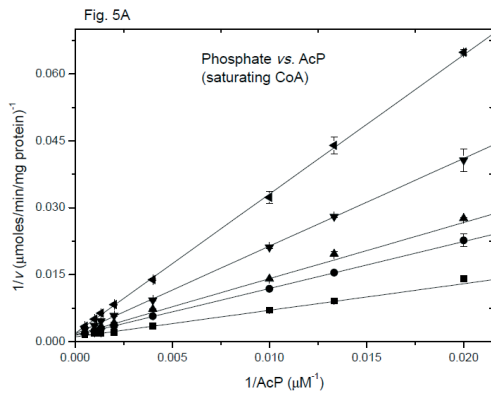


Figure 5. Product inhibition patterns for the reaction catalyzed by *S. saprophyticus* Pta. A, B and C, Phosphate concentration was kept constant at 0 mM (■), 5 mM (●), 10 mM (▲), 20 mM (▼) and 40 mM (◄). D and E, Acetyl-CoA concentrations were kept constant at 0 μM (■), 50 μM (●), 200 μM (▲), 500 μM (▼) and 1000 μM (◄). AcCoA, acetyl-CoA; AcP, acetyl phosphate. Other conditions as described in the "Experimental procedure" section.

Table 2. Product inhibition patterns of *S. saprophyticus* Pta and apparent inhibition constants, K_i . Apparent K_i values were calculated using Eqns 3 and 4 as described in Experimental procedures.

Inhibitor	Varied Substrate	Fixed Substrate	Inhibition pattern	Apparent K_i (mM)
Phosphate	acetyl~P	sat. CoA ^a	Competitive	12.0 ± 1.8
Phosphate	acetyl~P	subsat. CoA ^b	Competitive	8.6 ± 1.3
Phosphate	CoA	sat. acetyl~P ^c	No inhibition	-
Phosphate	CoA	subsat. acetyl~P ^d	Noncompetitive	8.2 ± 1.5
Acetyl-CoA	acetyl~P	sat. CoA ^a	No inhibition	-
Acetyl-CoA	acetyl~P	subsat. CoA ^b	Competitive	0.421 ± 0.072
Acetyl-CoA	CoA	sat. acetyl~P ^c	No inhibition	-
Acetyl-CoA	CoA	subsat. acetyl~P ^d	Competitive	0.321 ± 0.048

^aSaturating CoA (600 μM); ^bSubsaturating CoA (100 μM); ^cSaturating acetyl~P (4.0 mM); ^dSubsaturating acetyl~P (500 μM).

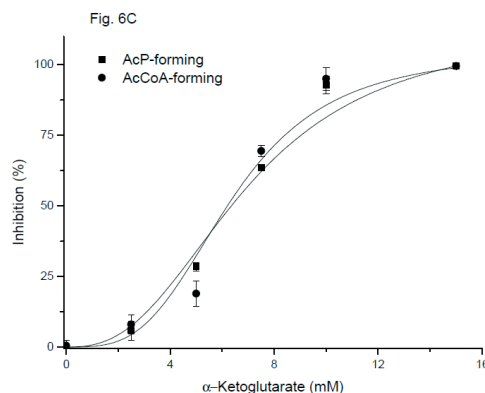
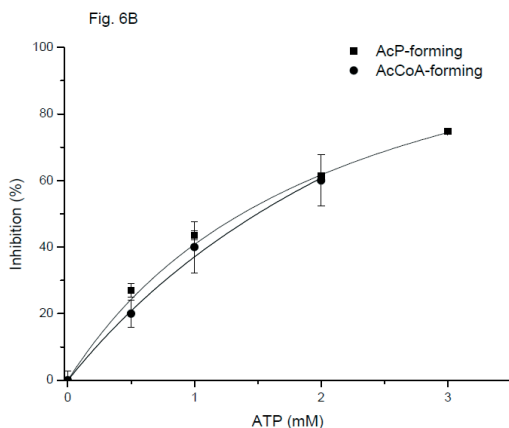
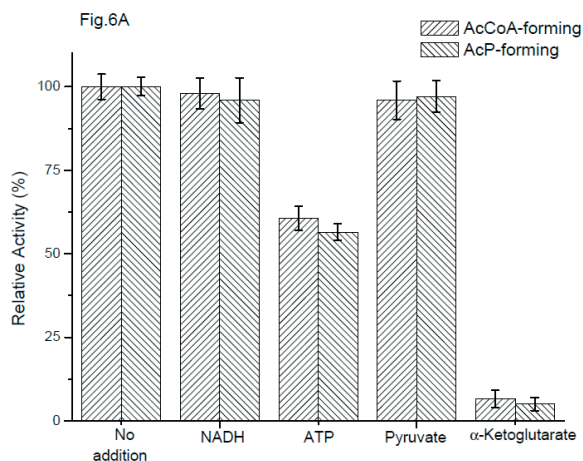


Figure 6. Effect of some metabolites on the activity of *S. saprophyticus* Pta in the acetyl-CoA (AcCoA)-forming (forward) or acetyl phosphate (AcP)-forming (reverse) directions. A, The activity of Pta in the forward and reverse reactions was monitored in the absence or presence of 1 mM NADH or ATP and 10 mM pyruvate or α-ketoglutarate. B and C, Inhibition of Pta activity in both forward and reverse directions by increasing concentrations of ATP and α-ketoglutarate, respectively. Results are presented as percentage inhibition in the presence of the effectors relative to the activity measured in the absence of the metabolites. Assays were performed at least in triplicate, and error bars indicate standard deviations. The solid lines indicate fitting the data to hyperbolic (B) or Hill equation (C).

phosphate-forming) directions. Pyruvate and NADH displayed no marked effect in either directions, but ATP and α -ketoglutarate were inhibitory (Fig. 6). The inhibition of Pta in both directions was analyzed at different concentrations of ATP and α -ketoglutarate (Figs. 6B and C). The inhibition by ATP was hyperbolic, whereas that by α -ketoglutarate was sigmoidal with half-saturations at about 6.5 ± 0.7 mM and Hill coefficients of 2.6 ± 0.8 and 3.3 ± 0.2 , in forward and reverse directions, respectively.

To determine the nature of inhibition by ATP, the velocity of the reaction was measured in the absence or presence of ATP and several concentrations of acetyl-P and CoA. The data, presented in the form of reciprocal plots (Fig. 7) show that the inhibition by ATP was competitive with respect to CoA and noncompetitive with respect to acetyl-P. The inhibition constants, K_i and βK_i , were 0.75 ± 0.15 mM and 2.75 ± 0.25 mM, respectively. This result further supports random binding suggested by the product inhibition pattern [12]. Due to allosteric nature of α -ketoglutarate inhibition it was complicated to determine its inhibition mechanism by the same way.

Discussion

Characterization of biochemical and kinetic properties of *S. saprophyticus* Pta

Here we cloned, expressed in *E. coli* and characterized the product of SSP2124 gene from uropathogenic *S. saprophyticus*. The recombinant enzyme displays a high phosphotransacetylase activity and appears to be similar to the other members of class I Ptas in terms of cation (K^+ or NH_4^+) requirements and inhibition by Na^+ ion (BRENDA database). Size exclusion chromatography studies revealed that *S. saprophyticus* Pta exist in solution as a dimer, which is consistent with the dimeric states observed for the crystal structures of PtaIs from *M. thermophila*, *B. subtilis*, and *S. pyogenes* [2, 11, 12]. Dilution of the enzyme to the concentration <0.005

mg/mL has resulted in a significant loss in the activity, suggesting that dimeric state is required for the activity.

The results of kinetic and end products inhibition analyses suggested that the kinetic mechanism proceeds through random formation of a ternary complex, which is in accord with the recent kinetic analyses of the recombinant Pta from *M. thermophila* as well as early kinetic analyses of Ptas purified from *V. alcalescens*, and *C. kluveri* [8, 11, 12]. Our results also indicate that in the forward reaction but not in the reverse direction binding of one substrate inhibits binding of the other ($\alpha \approx 4$). The apparent Michaelis constants of both CoA and acetyl-P increased approximately fourfold as the concentration of the corresponding second substrate was increased. These results are in good agreement with the results obtained with *C. kluveri* Pta by Henkin and Abeles [11].

The *S. saprophyticus* Pta activity was found to be sensitive to ATP but not affected by NADH and pyruvate. In this regard, it resembles the enzymes from *B. subtilis*, and *V. alcalescens*, which were also reported to be affected by ATP, but not by NADH and pyruvate [7, 8]. Our results also showed that the inhibition of *S. saprophyticus* Pta by ATP was competitive with respect to CoA and noncompetitive with respect to acetyl-P. Similar effect of ATP was found with *V. alcalescens* Pta [8], but in the case of *B. subtilis* Pta, kinetic analysis of ATP inhibition was not undertaken [7].

Allosteric inhibition of *S. saprophyticus* Pta activity by α -ketoglutarate

So far, only two PtaIIs from *E. coli* and *S. enterica* have been shown to be allosterically regulated via their N-terminal domains by NADH, ATP and pyruvate [5, 6]. In this study, we also first time showed that α -ketoglutarate, a substrate of α -ketoglutarate dehydrogenase complex (α -KGDC), one of the rate determining enzymes of TCA cycle, allosterically inhibited recombinant *S. saprophyticus* Pta activity

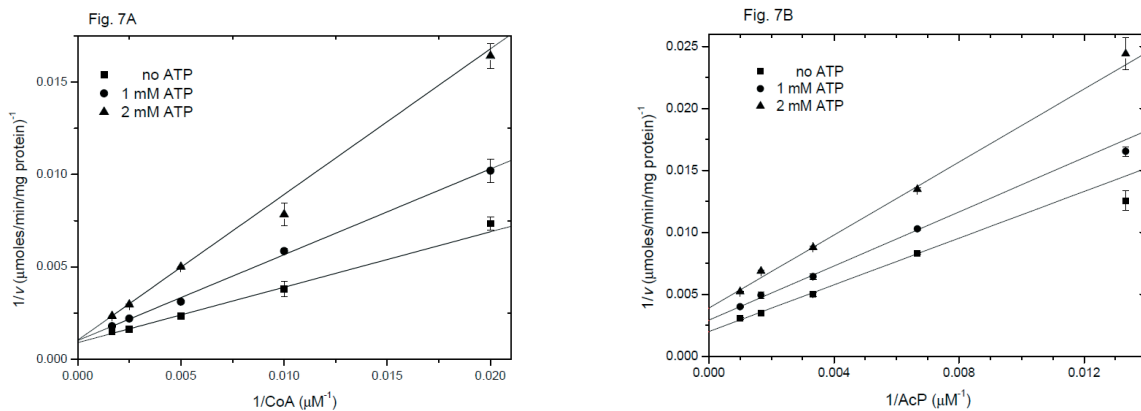


Figure 7. Reciprocal velocity of the forward reaction as a function of CoA (A) and acetyl phosphate (AcP) (B) concentrations in the absence and presence of indicated concentrations of ATP. AcP and CoA concentrations were kept constant at $500 \mu\text{M}$ (A) and $200 \mu\text{M}$ (B), respectively. Other conditions as described in the “Experimental procedure” section.

in both forward and reverse directions. A competition between Pta and α -KGDC for free CoA was proposed by El-Mansi [22] based on the ability of *E. coli* to accumulate α -ketoglutarate during growth on acetate. Pta out competes α -KGDC as it has lower K_m value for CoA, thus rendering α -KGDC rate-limiting in the Krebs cycle [22]. Since *S. saprophyticus* has not yet been studied in terms of determination of intermediates excreted during growth at different conditions, it is also not known whether *S. saprophyticus* accumulates α -ketoglutarate during growth on acetate. However, our data suggest that α -KGDC and Pta activities in *S. saprophyticus* are inversely regulated, and suppression of Pta activity by α -ketoglutarate ensures that α -KGDC wins the competition for free CoA.

In *E. coli*, the availability of oxygen regulates Pta, encoded by the *pta* gene, and α -KGDC expression levels [1, 23, 24]. Under anaerobic conditions, the levels of Pta as well as AckA increase about tenfold, whereas the expression of α -KGDC is severely inhibited [1, 23, 24]. Thus, in the absence of oxygen, in *E. coli* cells, the branched version of the TCA cycle is functional, and the cells generate ATP mainly by glycolysis and substrate phosphorylation via the Pta-AckA pathway [1]. As mentioned before, *E. coli* possesses both the *pta* and *eutD* genes, and the EutD protein has a high phosphotransacetylase activity and compensates lack of PtaII activity [4]. It would be interesting to see if α -ketoglutarate has any effect on PtaI activity.

Since the Pta we studied here is from *S. saprophyticus*, a Gram-positive bacterium, another Gram-positive bacterium *B. subtilis* is considered to be more useful paradigm; as a matter of fact not only for this case but for most of the Gram-positive bacterial world [25]. Besides, like *S. saprophyticus*, *B. subtilis* also has a PtaI. Pta plays a general role during anaerobic energy metabolism and contributes to aerobic growth of *B. subtilis* [1, 26-28]. Like *E. coli*, *B. subtilis* uses Pta-AckA pathway to convert acetyl-CoA to acetate via an acetyl~P intermediate, but, unlike *E. coli*, does not utilize the same pathway for growth on acetate [27]. Instead, it relies primarily on adenosine monophosphate (AMP)-forming acetyl-CoA synthetase (Acs; acetate:CoA ligase (AMP-forming), EC 6.2.1.1) [29]. Furthermore, the activity of Pta-AckA pathway as well as the expression of Pta in *B. subtilis* is unaffected by oxygen levels [28]. However, the expression and activity of α -KGDC as a function of oxygen levels have yet to be reported.

Significance of allosteric inhibition by α -ketoglutarate in relation to the physiological environment in the urinary tract

Obviously, the uropathogen *S. saprophyticus* is well adapted to the nutrient environment of urine, which contains high concentration of urea (~180 mM), ammonia (~20 mM) as well as an assortment of inorganic salts and organic compounds, including

amino acids and small peptides [30]. In addition, a urease, which catalyzes hydrolysis of urea, producing ammonia and carbon dioxide, has been implicated as one of the uropathogenic factors of *S. saprophyticus* [31]. Thus, nitrogen metabolism seems to be of importance for the survival of the cell. The role of α -ketoglutarate as a link between carbon and nitrogen metabolism in *B. subtilis* has been established [25, 32]. It activates GltC, a member of the LysR family of bacterial transcription factors, and the operon-specific regulator of *gltAB*, the gene encoding heterodimeric glutamate synthase (GOGAT) [32]. GOGAT catalyzes the synthesis of glutamate using α -ketoglutarate and glutamine as substrates. Glutamine is essential for cell growth as well as preferred nitrogen source of *B. subtilis* [29]. In *B. subtilis* glutamine synthetase is virtually the only enzyme that assimilates ammonium ions into organic compounds using α -ketoglutarate-glutamate-glutamine cycle [29]. Therefore, it seems likely that α -ketoglutarate-glutamate-glutamine cycle is effective in *S. saprophyticus* during urinary tract infection. The globular regulatory protein CodY, which is stimulated by GTP and branched-chain amino acids (BCAAs), activates *ackA* gene expression but represses *gltAB* [29, 33]. On the other hand, the transcription of *gltAB* is stimulated by another globular regulatory protein CcpA and glucose [34, 35]. CcpA also enhances expression of *pta* and *ackA* genes [36]. When the cells are exposed to glucose, CcpA regulates its own target genes and also those genes that are targets of CodY by stimulating the production of BCAAs [37, 38]. Thus, under conditions at which the *pta* and *gltAB* genes are coexpressed, α -ketoglutarate levels could play regulatory role in preserving acetyl~P levels by inhibiting Pta activity. As stated above, acetyl~P plays role in the regulation of more than 100 genes including those involved in nitrogen assimilation [1]. For instance, acetyl~P has been proposed to stimulate nitrogen assimilation by enhancing transcription of the *glnALG* operon, which encodes glutamine synthase in *E. coli* [39].

Human urine also contains D-serine at concentrations between 3 and 115 μ g/mL [40], which is toxic to some nonuropathogens but can be utilized or detoxified by uropathogenic *E. coli* CFT073. Welch and coworkers demonstrated that D-serine is preferentially consumed in tryptone broth by uropathogenic *E. coli* CFT073, and that the genes associated with acetate metabolism, including *ackA* and *pta* are upregulated, but *acs* is downregulated, following exposure to D-serine, which is catabolized into ammonia and pyruvate by serine deaminases [16]. Finally, the authors proposed that acetyl~P and acetyl-CoA whose intracellular levels are maintained by Pta and AckA play role in colonization of the urinary tract by CFT073 [16]. Sakinc *et al.* showed that *S. saprophyticus*, but not the other *Staphylococcus* species that do not possess D-serine deaminase, tolerates a high concentration of D-serine [41]. It is likely that a similar fate of D-serine

in this organism as in CFT073 takes place. The role of *S. saprophyticus* Pta, if there is any, in the metabolism of D-serine has yet to be elucidated.

Conclusion

In conclusion, here we first time characterized the recombinant *S. saprophyticus* Pta and investigated its kinetic mechanism, which turned out to occur via rapid equilibrium random model. Furthermore, we illustrated that it was allosterically inhibited by α -ketoglutarate, which is, to our best knowledge, the first example of allosteric regulation of a member of class I Ptas. However we have to emphasize that these studies were carried out using the recombinant Pta containing extra 20 amino acids including 6xHis residues coming from pET28a(+) expression vector, which we were not able to remove. Although it is less likely, these extra residues may play role in α -ketoglutarate effect. Studies on the elucidation of the mechanism of α -ketoglutarate action on *S. saprophyticus* Pta activity are underway.

Acknowledgements

We thank Dr. Ayhan Çelik for providing *Staphylococcus saprophyticus* genomic DNA.

References

- [1] Wolfe AJ. The acetate switch. *Microbiol. Mol Biol Rev* 2005; 69: 12-50.
- [2] Iyer PP, Lawrence SH, Luther KB, Rajashankar KR, Yennawar HP, Ferry JG, Schindelin H. Crystal structure of phosphotransacetylase from the methanogenic archaeon *Methanosarcina thermophila*. *Structure* 2004; 12: 559-567.
- [3] Lundie LL Jr, Ferry JG. Activation of acetate by *Methanosarcina thermophila*. Purification and characterization of phosphotransacetylase. *J Biol Chem* 1989; 264: 18392-18396.
- [4] Brinsmade SR, Escalante-Semerena JC. The eutD gene of *Salmonella enterica* encodes a protein with phosphotransacetylase enzyme activity. *J Bacteriol* 2004; 186: 1890-1892.
- [5] Brinsmade SR, Escalante-Semerena JC. In vivo and in vitro analyses of single-amino acid variants of the *Salmonella enterica* phosphotransacetylase enzyme provide insights into the function of its N-terminal domain. *J Biol Chem* 2007; 282: 12629-12640.
- [6] Campos-Bermudez VA, Bologna FP, Andreo CS, Drincovich MF. Functional dissection of *Escherichia coli* phosphotransacetylase structural domains and analysis of key compounds involved in activity regulation. *FEBS J* 2010; 277: 1957-1966.
- [7] Rado TA, Hoch JA. Phosphotransacetylase from *Bacillus subtilis*: Purification and physiological studies. *Biochim Biophys Acta* 1973; 321: 114-125.
- [8] Pelroy RA, Whiteley HR. Kinetic properties of phosphotransacetylase from *Veillonella alcalescens*. *J Bacteriol* 1972; 11: 47-55.
- [9] Xu QS, Shin D-H, Pufan R, Yokota H, Kim R, Kim S-H. Crystal structure of a phosphotransacetylase from *Streptococcus pyogenes*. *Proteins* 2004; 55: 479-481.
- [10] Xu QS, Jancarik J, Lou Y, Kusnetsova K, Yakunin AF, Yokota H, Adams P, Kim R, Kim S-H. Crystal structure of a phosphotransacetylase from *Bacillus subtilis* and its complex with acetyl phosphate. *J Struct Funct Genomics* 2005; 6: 269-279.
- [11] Henkin J, Abeles RH. Evidence against an acyl-enzyme intermediate in the reaction catalyzed by clostridial phosphotransacetylase. *Biochemistry* 1976; 15: 3472-3479.
- [12] Lawrence SH, Ferry JG. Steady-state kinetic analysis of phosphotransacetylase from *Methanosarcina thermophila*. *J Bacteriol* 2006; 188: 1155-1158.
- [13] Rasche ME, Smith KS, Ferry JG. Identification of cysteine and arginine residues essential for the phosphotransacetylase from *Methanosarcina thermophila*. *J Bacteriol* 1997; 179: 7712-7717.
- [14] Lawrence SH, Luther KB, Schindelin H, Ferry JG. Structural and functional studies suggest a catalytic mechanism for phosphotransacetylase from *Methanosarcina thermophila*. *J Bacteriol* 2006; 188: 1143-1154.
- [15] Bologna FP, Campos-Bermudez VA, Saavedra DD, Andreo CS, Drincovich MF. Characterization of *Escherichia coli* EutD: a phosphotransacetylase of the ethanolamine operon. *J Microbiol* 2010; 48: 629-636.
- [16] Anfora AT, Halladin DK, Haugen BJ, Welch RA. Uropathogenic *Escherichia coli* CFT073 is adapted to acetogenic growth but does not require acetate during murine urinary tract infection. *Infect Immun* 2008; 76: 5760-5767.
- [17] Kuroda M, Yamashita A, Hirakawa H, Kumano M, Morikawa K, Higashide M, Maruyama A, Inose Y, Matoba K, Toh H, Kuhara S, Hattori M, Ohta T. Whole genome sequence of *Staphylococcus saprophyticus* reveals the pathogenesis of uncomplicated urinary tract infection. *Proc Natl Acad Sci USA* 2005; 102: 13272-13277.
- [18] Segel IH. *Enzyme Kinetics: Behavior and analysis of rapid equilibrium and steady-state enzyme systems* 1993; John Wiley & Sons, Inc., New York.
- [19] Smith PK, Krohn RI, Hermanson GT, Mallia AK, Gartner FH, Provenzano MD, Fujimoto EK, Goetze NM, Olson BJ, Klenk DC. Measurement of protein using bicinchoninic acid. *Anal Biochem* 1985; 150: 76-85.
- [20] Laemmli UK. Cleavage of structural proteins during the assembly of the head of bacteriophage T4. *Nature* 1970; 227: 680-685.
- [21] Copeland RA. *Enzymes: A practical introduction to structure, mechanism, and data analysis*, 2000; Wiley-VCH, Inc. New York.
- [22] El-Mansi M. Free CoA-mediated regulation of intermediary and central metabolism: an hypothesis which accounts for the excretion of α -ketoglutarate during aerobic growth of *Escherichia coli* on acetate. *Res Microbiol* 2005; 156: 874-879.
- [30] Brooks T, Keevil CW. A simple artificial urine for the growth of urinary pathogens. *Lett Appl Microbiol* 1997; 24: 203-206.
- [31] Gatermann S, John J, Marre R. *Staphylococcus saprophyticus* urease: characterization and contribution to uropathogenicity in unobstructed urinary tract infection of rats. *Infect Immun* 1989; 57: 110-116.
- [32] Picossi S, Belitsky BR, Sonenshein AL. Molecular mechanism of the regulation of *Bacillus subtilis* *gluAB* expression by GluC. *J Mol Biol* 2007; 365: 1298-1313.
- [33] Shivers RP, Dineen SS, Sonenshein AL. Positive regulation of *Bacillus subtilis* *ackA* by CodY and CcpA: establishing a potential hierarchy in carbon flow. *Mol Microbiol* 2006; 62: 811-822.
- [34] Wacker I, Ludwig H, Reif I, Blencke H-M, Detsch C, Stülke J. The regulatory link between carbon and nitrogen metabolism in *Bacillus subtilis*: regulation of the *gluAB* operon by the catabolite control protein CcpA. *Microbiology* 2003; 149: 3001-3009.
- [35] Belitsky BR, Kim H-J, Sonenshein AL. CcpA-dependent regulation of *Bacillus subtilis* glutamate dehydrogenase gene expression. *J Bacteriol* 2004; 186: 3392-3398.

- [36] Moir-Blais TR, Grundy FJ, Henkin TM. Transcriptional activation of the *Bacillus subtilis ackA* promoter requires sequences upstream of the CcpA binding site. *J Bacteriol* 2001; 183: 2389–2393.
- [37] Shivers RP, Sonenshein AL. *Bacillus subtilis ilvB* operon: an intersection of global regulons. *Mol Microbiol* 2005; 56: 1549-1559.
- [38] Tojo S, Satomura T, Morisaki K, Deutscher J, Hirooka K, Fujita Y. Elaborate transcription regulation of the *Bacillus subtilis ilv-leu* operon involved in the biosynthesis of branched-chain amino acids through global regulators of CcpA, CodY and TnrA. *Mol Microbiol* 2005; 56: 1560-1573.
- [39] Feng J, Atkinson MR, McCleary W, Stock JB, Wanner BL, Ninfa AJ. Role of metabolic intermediates in the regulation of glutamine synthetase synthesis in *Escherichia coli*. *J Bacteriol* 1992; 174: 6061-6070.
- [40] Huang Y, Nishikawa T, Satoh K, Iwata T, Fukushima T, Santa T, Homma H, Imai K. Urinary excretion of D-serine in human: comparison of different ages and species. *Biol Pharm Bull* 1998; 21: 156-162.
- [41] Sakinç T, Michalski N, Kleine B, Gatermann SG. The uropathogenic species *Staphylococcus saprophyticus* tolerates a high concentration of D-serine. *FEMS Microbiol Lett* 2009; 299: 60-64.

Footnotes

¹Although the genes encoding PtaIs are designated as *eutD* gene, which is a member of *eut* operon encoding proteins involved in ethanolamine metabolism, not all PtaI genes are located in a *eut* operon; as a matter of fact, some microorganism do not even have ethanolamine utilization operon (KEGG database).